A Journal of the Gesellschaft Deutscher Chemiker
Angewandte Chemie
GDCh
International Edition
www.angewandte.org

Title: Integrating Biomass into Organonitrogen Chemical Supply Chain: Production of Pyrrole and D-Proline from Furfural

Authors: Song Song, Vincent Fung Kin Yuen, Lu Di, Qiming Sun, Kang Zhou, and Ning Yan

To be cited as: *Angew. Chem. Int. Ed.* 10.1002/anie.202006315

Link to VoR: https://doi.org/10.1002/anie.202006315

WILEY-VCH

Integrating Biomass into Organonitrogen Chemical Supply Chain: Production of Pyrrole and D-Proline from Furfural

Song Song, Vincent Fung Kin Yuen, Lu Di, Qiming Sun, Kang Zhou,* and Ning Yan*

Abstract: Production of renewable, high-value N-containing chemicals from lignocellulose will expand product diversity and increase the economic competitiveness of biorefinery. Herein, we report a single-step conversion of furfural to pyrrole in 75% yield as a key N-containing building block, achieved via tandem decarbonylation-amination reactions over tailor-designed Pd@S-1 and H-beta zeolite catalytic system. Pyrrole was further transformed into DL-proline in two steps following carboxylation with CO_2 and hydrogenation over Rh/C catalyst. After treating with *Escherichia coli*, valuable D-proline was obtained in theoretically maximum yield (50%) bearing 99% ee. The report here establishes a route bridging commercial commodity feedstock from biomass with high-value organonitrogen chemicals through pyrrole as a hub molecule.

Lignocellulose is the most abundant and renewable biomass on Earth. Previous work mainly focused on the production of various hydrocarbons and oxygen-containing chemicals.[1] Expanding the product scope beyond C-, O-, H- bearing compounds will diversify the biorefinery economy. Nitrogen-containing chemical synthesis *via* C-N bond formation represents a new opportunity in biomass valorization due to the nitrogen deficient nature of lignocellulose. There have been excellent advances along this direction in recent years,[2] but more remain to be developed considering the large number of organonitrogen chemicals used in industry and daily life.

The main pathway to make organonitrogen chemicals in current industry involves C-H activation of hydrocarbons to introduce oxygen functionality followed by incorporation of nitrogen functionalities to obtain N-containing chemicals. These primary organonitrogen chemicals serve as building blocks for a broad range of downstream products. Pyrrole is an important primary N-containing chemical extensively used as precursors for fine chemicals, drugs, catalysts and materials.[3] The classic protocol for pyrrole synthesis is through oxidation of 1,3-butadiene into furan followed by an additional amination reaction.[4] Starting from chitin, pyrrole was also obtained but the yield was only around 10%.[5]

In the downstream side of the organonitrogen chemical supply chain, L/D-proline[6] is a representative example extensively used either directly,[7] or as precursor for pharmaceuticals. Its market is expected to grow at an annual rate of 5.3% over the next five years, and to reach US$ 310 million in 2025.[8] Industrially, L-proline is produced *via* fermentation with glucose as the substrate.[9] However, no fermentation process has been reported for direct D-proline production. Racemic proline can be chemically synthesized from petroleum-based diethyl malonate with acrylonitrile through complex processes with at least 5 steps. At present, renewable and cost-effective method for D-proline production is scarce. Since D-proline is a critical precursor for important chemicals such as (-)-secu’amamine A and (*R*)-harmicine,[10] and is a useful catalyst to access many chiral molecules,[11] new protocols for producing D-proline from renewable starting materials is desirable.

Bio-based furans, being commercially available and affordable (e.g., 1.1-1.3 US$ kg^{-1} for furfural),[12] are among the most promising feedstock to establish the organonitrogen chemical supply chain in biorefinery. The structural similarity of pyrrole and D-proline with furans prompted us to explore chemical routes to bridge them. Herein, we communicate the direct transformation of furfural into pyrrole, which, as a hub molecule, is further converted into high-value D-proline (Figure. 1). For pyrrole synthesis, aldehyde groups in furfural are removed and oxygen in the furan ring is replaced by nitrogen using NH_3 *via* one-step decarbonylation-amination reaction over a tailor-designed catalytic system. Following carboxylation using CO_2 and hydrogenation of the furan ring, racemic proline was obtained in high yield, which was kinetically resolved with *E. coli* to produce pure D-proline.

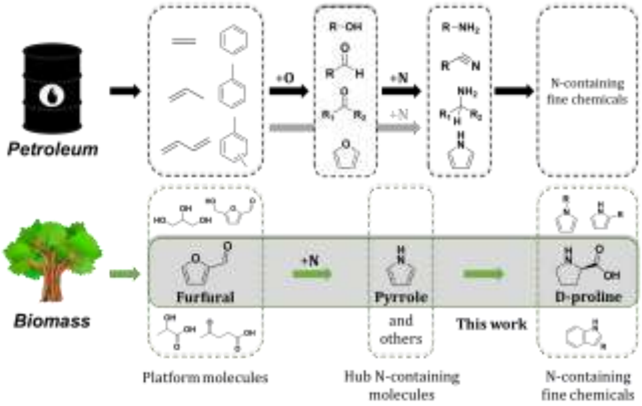

Figure 1. A simplified overview of how organochemicals are made from petroleum resources, the proposed organonitrogen chemical supply chain in biorefinery, and the scope of current work.

---

[*] Dr. S. Song, V. Fung, Dr. Q. Sun, Prof. Dr. K. Zhou, Prof. Dr. N. Yan
Department of Chemical & Biomolecular Engineering
National University of Singapore
4 Engineering Drive 4, Singapore 117585 (Singapore)
E-mail: ning.yan@nus.edu.sg
E-mail: kang.zhou@nus.edu.sg
Dr. L. Di
School of Materials Science and Engineering
Nankai University
38 Tongyan Road, Haihe Educational Park, Tianjin 300350 (P. R. China)
Supporting information for this article is given via a link at the end of the document.

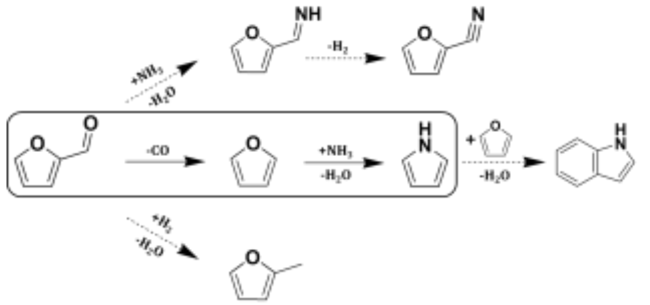

Scheme 1. Reaction network for single-step conversion of furfural to pyrrole in the presence of NH_3 and H_2.

To our knowledge, single-step decarbonylation-amination of furfural into pyrrole in the presence of NH_3 and H_2 (Scheme 1) has not been achieved so far. Previously, Pd-based catalysts have been reported effective for furfural decarbonylation to furan,[13] but the effect of NH_3 remains unknown. Thus, we started by comparing furfural decarbonylation in the absence and presence of NH_3. Several commercial and home-made Pd-catalysts (Pd/TiO_2, Pd/SiO_2, Pd/Al_2O_3, Pd/AC and Pd@S-1) were tested. The major difference between the first four catalysts and the last Pd@S-1 catalyst is that Pd NPs are exposed on the exterior surface of supports in the former, while encapsulated and confined in the zeolite pores in the latter (see graphic views in Figure 2a-2b). In the absence of NH_3, >90% furfural conversion and ~90% furan selectivity were observed over Pd/SiO_2, Pd/Al_2O_3, Pd/AC and Pd@S-1 catalysts under optimized condition, while Pd/TiO_2 provided substantially lower conversion (41%) and exclusive formation of 2-methylfuran as an undesired product (Figure 2c, S1 and Scheme S1). The strong metal-support interaction (SMSI) over Pd/TiO_2, as observed in XPS analysis (Figure S2), may change the furfural adsorption mode, thereby switching the reaction pathway from decarbonylation to hydrodeoxygenation (Figure 2c).

Significant catalyst deactivation was observed over all four supported Pd catalysts after the injection of NH_3 (Figure 2d). The furfural conversion decreased from 92%, 100% and 100% to 65%, 80% and 97% over Pd/SiO_2, Pd/Al_2O_3 and Pd/AC catalysts, respectively, after 3 h time-on-stream (TOS), and decreased further after 6 h TOS (Figure S3). The loss in catalytic activity is partially attributed to competitive adsorption of NH_3 as suggested by in situ FTIR study using CO as a probe molecule (Figure S4), and partially to the increase of coke formation in the presence of NH_3, as evidenced by thermogravimetric analysis (TGA) (Figure S5). The amount of coke formation in Pd/SiO_2 catalyst in the presence of NH_3 was almost 3 times higher compared to that without NH_3. Similarly, the coke amount increased around 30% over Pd/Al_2O_3 catalyst after introducing NH_3. The product distributions also changed significantly. When NH_3 was added, 2-furonitrile and 2-methylfuran appeared as main side products over Pd/TiO_2, Pd/SiO_2, Pd/Al_2O_3 and Pd/AC catalysts (Figure 2d). The formation of 2-furonitrile could be due to the loss in decarbonylation activity and consequently the unconverted furfural reacted with NH_3 to form imine and finally nitriles. The selectivity toward 2-methylfuran increased after introducing NH_3, especially for the Pd/AC catalyst. During furfural decarbonylation, the furan ring was strongly adsorbed on the Pd surface. However, the preferential adsorption of aldehyde group on Pd surface may be enhanced after NH_3 injection, which increased the hydrodeoxygenation of furfural to 2-methylfuran.[14]

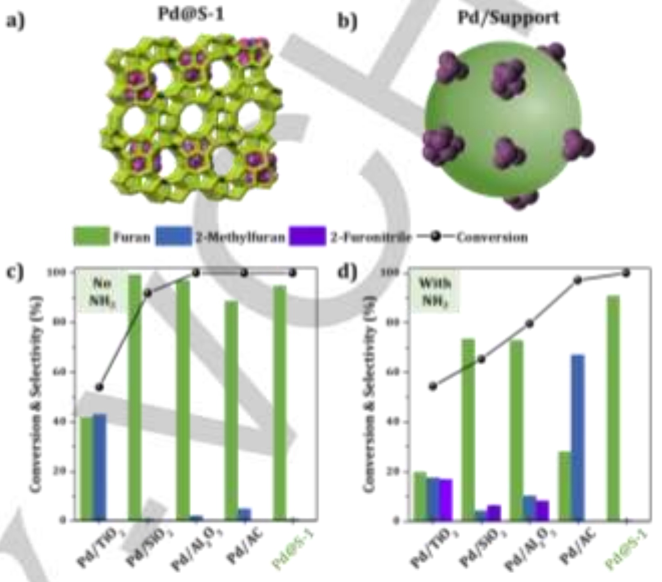

Figure 2. Graphic view of Pd@S-1 and other Pd-based catalysts. a) Pd@S-1; b) Pd on other supports. NH_3 effect on conversion (dots) and product distribution (bars) for gas-phase furfural decarbonylation. c) No NH_3; d) With NH_3. Reaction conditions: catalyst 100 mg, furfural weight hourly space velocity (WHSV) = 0.2 h^{-1}, NH_3 0 or 4 ml/min, H_2 20 ml/min, T = 350 °C, 1 bar, TOS = 3 h.

Encapsulation of ultra-small metal nanoparticles inside zeolite channels to form core-shell structures (metal@zeolite) is an effective strategy for synthesizing highly selective and active metal catalysts.[15] In opposition to the fast deactivation and low selectivity of commercial Pd catalyst in furfural decarbonylation in the presence of NH_3, NH_3 had little influence on the catalytic performance of Pd@S-1 (Figure 2c, 2d). The furan yield remained >90%. TGA results showed that Pd@S-1 catalyst was highly resistant against coke formation (< 1%) regardless of the NH_3 concentration in the feed, which explains the stable catalytic activity (Figure S5). The lower coke formation over Pd@S-1 catalyst was mainly attributed to the negligible acidity nature of the silica support, the suitable pore channel structure for furans to diffuse,[13a] and its exceptional NH_3-resistant activity. The high selectivity towards furan in the presence of NH_3 may also due to the pore confinement effect.[13a] No obvious Pd metal particle aggregation was observed after reaction or regeneration (Figure S6). From above, Pd@S-1 is a robust and suitable catalyst for furfural decarbonylation to furan under NH_3 atmosphere compared to common, commercially available Pd catalysts.

Next, we studied the one-step conversion of furfural to pyrrole. Considering the amination of furan to pyrrole is promoted by acids, different types of solid acid catalysts, including γ-Al_2O_3, SiO_2-Al_2O_3, HZSM-5, H-beta and H-USY, were chosen and combined with Pd@S-1 to demonstrate the viability of the single-

10.1002/anie.202006315

Table 1: Conversions and product distributions over different catalyst combinations for one-step furfural to pyrrole.

Entry	Cat. 1	Cat. 2	Conv. [%]	Product selectivity [%]				Carbon balance [%]
				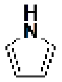	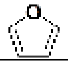		Others	
1[a]	Pd@S-1	None	100	0	91	0	9	90
2[b]	Pd@S-1	SiO_2-Al_2O_3 (1.8)[c]	100	11	74	0	15	89
3[b]	Pd@S-1	γ-Al_2O_3	100	5	81	0	14	87
4[b]	Pd@S-1	H-beta (25)[c]	100	75	13	0	12	89
5[b]	Pd@S-1	H-ZSM-5 (25)[c]	100	60	23	6	11	86
6[b]	Pd@S-1	H-USY (14)[c]	100	42	45	7	6	83

[a] Reaction conditions: 100 mg catalyst 1, furfural WHSV = 0.2 h^{-1}, H_2 20 ml/min, T = 350 °C, 1 bar, TOS = 3 h. [b] Reaction conditions: 100 mg catalyst 1, 100 mg catalyst 2, furfural WHSV = 0.1 h^{-1}, NH_3 12 ml/min, H_2 20 ml/min, T = 460 °C, 1 bar, TOS = 3 h. [c] SiO_2/Al_2O_3 ratio.

step conversion strategy. Furan amination required 400-450 °C to occur,[16] but higher temperature (> 350 °C) was not suitable for furfural decarbonylation. Almost 40% carbon was lost when the reaction temperature was 400 °C (Figure S1). Hence, Pd@S-1 and solid acid catalysts were loaded into two different zones in the fixed-bed reactor to satisfy reaction conditions required for each step, with detailed scheme shown in Figure S7. With the adoption of dual layers in which the solid acid catalyst layer has a higher temperature than the Pd@S-1 layer, the carbon balance reached ~90% (Table 1). No pyrrole was observed in the absence of acid catalyst (Table 1, entry 1), while its selectivity was only 5% and 11% over γ-Al_2O_3 and SiO_2-Al_2O_3 catalysts, respectively (Table 1, entries 2-3). Zeolites exhibited much higher activities than γ-Al_2O_3 and SiO_2-Al_2O_3 (Table 1, entries 4-6). Based on the NH_3 temperature-programmed desorption, zeolites were more acidic than γ-Al_2O_3 and SiO_2-Al_2O_3 (Figure S8) explaining the better performance. Indole was detected as a side product when HZSM-5 or HUSY was used, which formed via the Diels-Alder and dehydration reactions between furan and pyrrole. The highest pyrrole selectivity (75%) was observed over H-beta, possibly due to its medium acidity among the selected solid acid catalysts. In a continuous test of 12 h, furfural conversion was stable and pyrrole selectivity decreased slightly from 75% to 60% over the Pd@S-1/H-beta multifunctional catalytic system. After regeneration at 550 °C for 4 h in air, the system fully resumed its original catalytic activity (Figure S9).

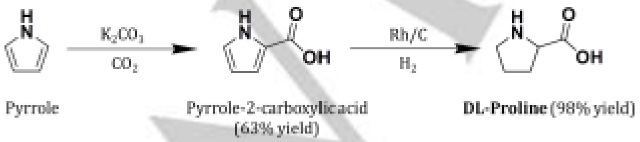

Figure 3. Conversion of pyrrole to racemic proline. Carboxylation reaction condition: pyrrole 2 mmol, K_2CO_3 10 mmol, H_2O 2 mL, initial CO_2 70 bar, T = 100 °C, t = 24 h. Hydrogenation reaction condition: pyrrole-2-carboxylic acid 2 mmol, Rh/C 20 mg, *i*-PrOH 3 mL, H_2 30 bar, T = 100 °C, t = 24 h.

To demonstrate biomass derived pyrrole could serve as a hub molecule to access more value-added chemicals, we designed a two-step protocol to convert pyrrole into DL-proline (Figure 3). The first step is base-promoted carboxylation using CO_2, which has been studied but the product yield was around 40%.[17] We tested the effectiveness of different inorganic bases (Table S5, entries 1-8), and the best activity was observed when K_2CO_3 was used, affording 21% pyrrole-2-carboxylic acid after 3 h at 120 °C under 40 bar CO_2. Prolonging the reaction time to 24 h, the yield increased to 32% (Table S5, entry 9). The effect of reaction temperature and initial CO_2 pressure were further evaluated (Table S5, entries 9-15). The product yield increased from 32% to 36% upon reducing the temperature from 120 °C to 100 °C, but dropped to 20% when further decreasing temperature to 80 °C. A volcano-type activity trend was also observed for initial CO_2 pressure (Table S5, entries 11-15). At 20 bar, the yield of pyrrole-2-carboxylic acid was 28%. Increasing the pressure to 55 bar and 70 bar, 45% and 63% yields were obtained, respectively. The yield decreased to 38% when increasing the initial CO_2 pressure to 90 bar. Thus, the highest yield of pyrrole-2-carboxylic acid obtained from the carboxylation of pyrrole with CO_2 was 63%. Following that, quantitative yield of racemic DL-proline (98%) was obtained by hydrogenation using a commercial Rh/C catalyst.

Since D-proline can not be directly obtained via the current fermentation technologies, the kinetic resolution of DL-proline was performed to remove L-proline from the mixture. We chose *E. coli* for this study as it is a well-studied model micro-organism, and it has been used to produce organonitrogen chemicals from renewable feedstocks.[18] L-proline, but not D-proline, can serve as a sole carbon and nitrogen source for wildtype *E. coli*.[19] Wild-type *E. coli* contains a three-step L-proline utilization pathway, which oxidises L-proline to L-glutamate. L-proline oxidation to L-glutamate is catalysed by proline utilization A (PutA) protein, which has both proline dehydrogenase and L-glutamate-5-semialdehyde dehydrogenase activities (Figure 4a).[20] L-glutamate is further deaminated into α-ketoglutarate. Here, the carbon flux can then be further directed to gluconeogenesis and the pentose phosphate pathway, which are critical in producing important building blocks for biomass formation. When biomass accumulates, more PutA are expressed to consume L-proline, leaving D-proline behind. We inoculated wildtype *E. coli* BL21(DE3) strain in a chemically defined medium with commercially available L-proline, D-proline or DL-proline (5 g/L each) as the sole carbon source (Figure 4b, S10-S11). After a 48-h aerobic incubation at 37 °C, L-proline was fully consumed and cell density (OD_{600}) of the *E. coli* strain reached ~3.8, while the yield of D-proline from the kinetic resolution process was 99.4% (Figure 4b). Acetate, a commonly encountered aerobic fermentation product, was not detected (detection limit: 0.1 g/L). Based on materials balance, the consumed L-proline should be converted into CO_2 and biomass (e.g. nucleic acids, proteins and lipids). As such, an effective kinetic resolution of DL-proline by using *E. coli* fermentation is developed.

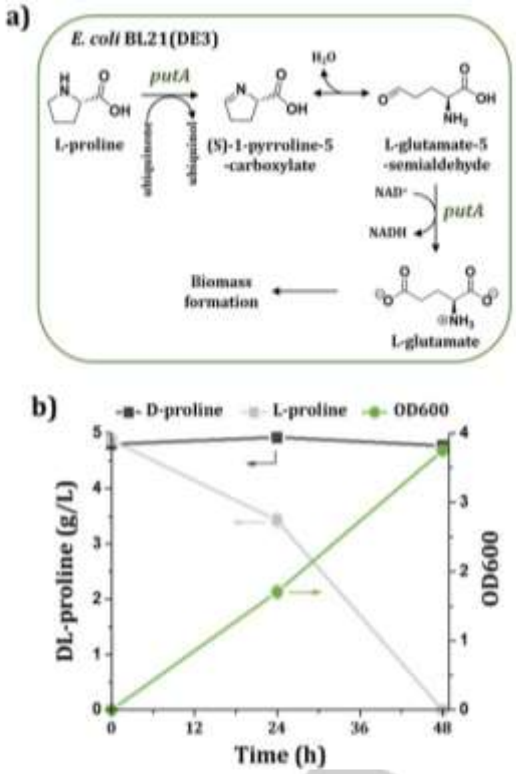

Figure 4. Kinetic resolution of DL-proline. a) The schematic drawing of consuming L-proline from DL-proline in wild-type *E. coli* BL21(DE3); b) DL-proline as substrate. The size of the error bars (SE, n=2) is smaller than the symbol sizes. Experiments were performed as descirbed in Section 1.5 in SI.

We further demonstrated the integration of chemical and biological steps. The isolated DL-proline from pyrrole-2-carboxylic acid hydrogenation was used in the biological step to produce D-proline. After 48 h, L-proline was depleted while no D-proline was consumed, highlighting chemical and biological transformations established in this study can be seamlessly combined. (Figure S12).

If the production of L-proline is desired, D-proline can be converted into L-proline via an imino acid by simultaneously using a proline oxidase that only accepts D-proline as the substrate, and sodium cyanoborohydride which reduces the imino acid into DL-proline.[21] We validated the method by using commercially available DL-proline (yield: 81%; ee >99%; Figure S13). As such, two kinetic resolution methods are established to obtain D- and L-proline, respectively.

To summarize, we have developed renewable routes to produce two value-added nitrogen-containing chemicals pyrrole and D-proline from biomass-derived furfural via decarbonylation-amination, carboxylation, hydrogenation and kinetic resolution. This work showcases the possibility of establishing organonitrogen chemical supply chain in biorefinery, via the transformation of biomass derived feedstock into hub organochemcials that can be diversified into a spectrum of end products. It also provides an example for recovering original stereo-structure of biomass, which was lost during the traditional treatment process. A limitation of the current work is the loss of CO (20% of carbon) in the first step. We attempted to produce proline from 2-furoic acid and 2-methylfuran to prevent carbon loss, but these two routes, so far, have not been successful under applied conditions (Figure S14).

Acknowledgements

The authors thank the Tier-1 & Tier-2 projects from Singapore Ministry of Education (R-279-000-462-112, R-279-000-479-112 and R-279-000-594-112) and the C4T Emerging Opportunities Fund - EOF2 from Cambridge Centre for Advanced Research and Education in Singapore Ltd (CARES) (R-279-000-604-592). Dr. L. Di thanks the National Natural Science Foundation of China (Grant 21905144). We thank Daniel Tan, Jeff Zhou, Smaranika Panda and You-Kang Lim (NUS) for their assisstance on the kinetic resolution experiments, as well as Prof. Alexei A Lapkin and Dr. Zhen Guo (Cambridge & NUS) for inspirational discussions.

Keywords: furfural • pyrrole • proline • decarbonylation-amination • kinetic resolution

[1] a) A. Corma, S. Iborra, A. Velty, *Chem. Rev.* **2007**, *107*, 2411-2502; b) G. W. Huber, S. Iborra, A. Corma, *Chem. Rev.* **2006**, *106*, 4044-4098; c) W. Schutyser, T. Renders, S. Van den Bosch, S.-F. Koelewijn, G. Beckham, B. F. Sels, *Chem. Soc. Rev.* **2018**, *47*, 852-908; d) X. Wu, X. Fan, S. Xie, J. Lin, J. Cheng, Q. Zhang, L. Chen, Y. Wang, *Nat. Catal.* **2018**, *1*, 772-780; e) L. Dong, L. Lin, X. Han, X. Si, X. Liu, Y. Guo, F. Lu, S. Rudic, S. F. Parker, S. Yang, Y. Wang, *Chem* **2019**, *5*, 1521-1536.

[2] a) E. M. Karp, T. R. Eaton, V. S. i Nogué, V. Vorotnikov, M. J. Biddy, E. C. Tan, D. G. Brandner, R. M. Cywar, R. Liu, L. P. Manker, W. E. Michener, M. Gilhespy, Z. Skoufa, M. J. Watson, O. S. Fruchey, D. R. Vardon, R. T. Gill, A. D. Bratis, G. T. Beckham, *Science* **2017**, *358*, 1307-1310; b) G. Liang, A. Wang, L. Li, G. Xu, N. Yan, T. Zhang, *Angew. Chem. Int. Ed.* **2017**, *56*, 3050-3054; c) M. Pelckmans, W. Vermandel, F. Van Waes, K. Moonen, B. F. Sels, *Angew. Chem. Int. Ed.* **2017**, *56*, 14540-14544; d) W. Deng, Y. Wang, S. Zhang, K. M. Gupta, M. J. Hülsey, H. Asakura, L. Liu, Y. Han, E. M. Karp, G. T. Beckham, P. J. Dyson, J. Jiang, T. Tanaka, Y. Wang, N. Yan, *Proc. Natl. Acad. Sci.* **2018**, *115*, 5093-5098; e) I. Scodeller, S. Mansouri, D. Morvan, E. Muller, K. de Oliveira Vigier, R. Wischert, F. Jérôme, *Angew. Chem. Int.*

Ed. **2018**, *57*, 10510-10514; f) A. Afanasenko, T. Yan, K. Barta, *Commun. Chem.* **2019**, *2*, 127; g) C. Xie, J. Song, H. Wu, Y. Hu, H. Liu, Z. Zhang, P. Zhang, B. Chen, B. Han, *J. Am. Chem. Soc.* **2019**, *141*, 4002-4009; h) H. Li, H. Guo, Y. Su, Y. Hiraga, Z. Fang, E. J. Hensen, M. Watanabe, R. L. Smith, *Nat. Commun.* **2019**, *10*, 699; i) Y. Wang, S. Furukawa, S. Song, Q. He, H. Asakura, N. Yan, *Angew. Chem. Int. Ed.* **2020**, *59*, 2289-2293.

[3] S. Michlik, R. Kempe, *Nat. Chem.* **2013**, *5*, 140-144.

[4] K. Hatada, M. Shimada, K. Fujita, Y. Ono, T. Keii, *Chem. Lett.* **1974**, *3*, 439-442.

[5] X. Gao, X. Chen, J. Zhang, W. Guo, F. Jin, N. Yan, *ACS Sustain. Chem. Eng.* **2016**, *4*, 3912-3920.

[6] L. Szabados, A. Savoure, *Trends Plant Sci.* **2010**, *15*, 89-97.

[7] B. List, R. A. Lerner, C. F. Barbas, *J. Am. Chem. Soc.* **2000**, *122*, 2395-2396.

[8] *Marketwatch.com, 'Global proline market is projected to reach at a CAGR of 5.3% during 2020-2025: Eon Market Research', 2020. [Online]. Available: https://www.marketwatch.com/story/global-proline-market-is-projected-to-reach-at-a-cagr-of-53-during-2020-2025-eon-market-research-2020-04-06.*

[9] K. Araki, Y. Takasawa, J. Nakajima, *Agric. Biol. Chem.* **1975**, *39*, 1193-1200.

[10] a) P. Liu, S. Hong, S. M. Weinreb, *J. Am. Chem. Soc.* **2008**, *130*, 7562-7563; b) C. S. Lood, A. M. Koskinen, *Eur. J. Org. Chem.* **2014**, *2014*, 2357-2364.

[11] D. Mandalapu, *Synlett* **2015**, *26*, 707-708.

[12] a) R. Mariscal, P. Maireles-Torres, M. Ojeda, I. Sádaba, M. L. Granados, *Energy Environ. Sci.* **2016**, *9*, 1144-1189; b) Y. Nakagawa, K. Takada, M. Tamura, K. Tomishige, *ACS Catal.* **2014**, *4*, 2718-2726; c) N. Luo, T. Montini, J. Zhang, P. Fornasiero, E. Fonda, T. Hou, W. Nie, J. Lu, J. Liu, M. Heggen, L. Lin, C. Ma, M. Wang, F. Fan, S. Jin, F. Wang, *Nat. Energy* **2019**, *4*, 575-584.

[13] a) C. Wang, L. Wang, J. Zhang, H. Wang, J. P. Lewis, F. Xiao, *J. Am. Chem. Soc.* **2016**, *138*, 7880-7883; b) W. Zhang, Y. Zhu, S. Niu, Y. Li, *J. Mol. Catal. A: Chem.* **2011**, *335*, 71-81.

[14] a) V. Vorotnikov, G. Mpourmpakis, D. G. Vlachos, *ACS Catal.* **2012**, *2*, 2496-2504; b) S. H. Pang, C. A. Schoenbaum, D. K. Schwartz, J. W. Medlin, *Nat. Commun.* **2013**, *4*, 2448.

[15] a) N. Wang, Q. Sun, J. Yu, *Adv. Mater.* **2019**, *31*, 1803966; b) S. M. Wu, X. Y. Yang, C. Janiak, *Angew. Chem. Int. Ed.* **2019**, *58*, 12340-12354; c) Y. Chai, W. Shang, W. Li, G. Wu, W. Dai, N. Guan, L. Li, *Advanced Science* **2019**, *6*, 1900299.

[16] L. Tao, Z. Wang, T. Yan, Y. Liu, H. He, Y. Cao, *ACS Catal.* **2016**, *7*, 959-964.

[17] a) E. Smissman, M. Graber, R. Winzler, *J. Am. Pharm. Assoc.* **1956**, *45*, 509; b) A. Radhakrishnan, A. Meister, *J. Biol. Chem.* **1957**, *226*, 559-571.

[18] X. Ma, G. Gözaydın, H. Yang, W. Ning, X. Han, N. Y. Poon, H. Liang, N. Yan, K. Zhou, *Proc. Natl. Acad. Sci.* **2020**, *117*, 7719-7728.

[19] a) J. M. Wood, *J. Bacteriol.* **1981**, *146*, 895-901; b) H. Sasaki, A. Takaki, A. Oshima, A. Ishida, S. Nagata, *Ann. Microbiol.* **2007**, *57*, 265.

[20] Y. Zhou, W. Zhu, P. S. Bellur, D. Rewinkel, D. F. Becker, *Amino Acids* **2008**, *35*, 711-718.

[21] T. M. Beard, N. J. Turner, *Chem. Commun.* **2002**, *3*, 246-247.

Entry for the Table of Contents (Please choose one layout)

Layout 1:

COMMUNICATION

Nitrogen-containing chemicals: Production of renewable nitrogen-containing chemicals (Pyrrole and D-proline) from biomass-derived furfural is achieved through a protocol combining chemical and biological process.

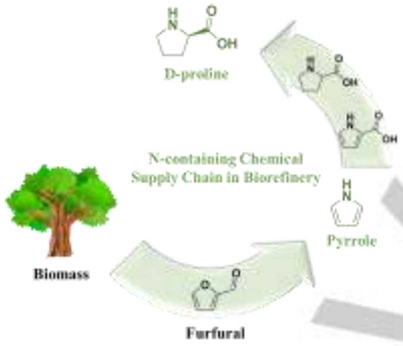

S. Song, V. Fung, L. Di, Q. Sun, K. Zhou, N. Yan**

Page No. – Page No.

Integrating Biomass into Organonitrogen Chemical Supply Chain: Production of Pyrrole and D-Proline from Furfural